Navigation Accuracy and Interference Rejection for an Adaptive GPS Antenna Array

David S. De Lorenzo, *Stanford University*
Jason Rife, *Stanford University*
Per Enge, *Stanford University*
Dennis M. Akos, *University of Colorado*

BIOGRAPHY

David De Lorenzo is a member of the Stanford University GPS Laboratory, where he is pursuing a Ph.D. degree in Aeronautics and Astronautics. He received a Master of Science degree in Mechanical Engineering from the University of California, Davis, in 1996. David has worked previously for Lockheed Martin and for the Intel Corporation.

Dr. Jason Rife is a Research Associate studying JPALS and the Local Area Augmentation System (LAAS) at Stanford University. After receiving his B.S. in Mechanical and Aerospace Engineering from Cornell University (1996), he spent one year working in the turbine aerodynamics group of the commercial engine division of Pratt & Whitney. He resumed his studies at Stanford and earned M.S. (1999) and Ph.D. (2004) degrees in Mechanical Engineering. His thesis work focused on positioning and navigation technologies for underwater robots.

Dr. Per Enge is a Professor of Aeronautics and Astronautics at Stanford University, where he is the Kleiner-Perkins, Mayfield, Sequoia Capital Professor in the School of Engineering. He directs the GPS Research Laboratory, which develops satellite navigation systems based on the Global Positioning System. Dr. Enge has received the Kepler, Thurlow, and Burka Awards from the Institute of Navigation for his work. He is a Fellow of the Institute of Navigation and the Institute of Electrical and Electronics Engineers.

Dr. Dennis M. Akos is an Assistant Professor with the Aerospace Engineering Science Department at the University of Colorado at Boulder. He also has served as a faculty member with the Luleå Technical University, Sweden, and as a Research Associate in the GPS Laboratory at Stanford University. Dr. Akos completed the Ph.D. degree in Electrical Engineering at Ohio University within the Avionics Engineering Center.

ABSTRACT

In the Joint Precision Approach and Landing System (JPALS) both the differential GPS reference station and the airborne user will employ Controlled Reception Pattern Array (CRPA) antennas. In a high precision system such as JPALS, CRPA antennas may suffer phase center biases that introduce significant integrity risk. These phase center biases result from both hardware design and from algorithm selection (beamsteering and/or nullforming). This study shows that there is a clear trade-off between radio frequency interference (RFI) rejection and the introduction of biases in the pseudorange and carrier-phase navigation outputs from a space-time adaptive processor (STAP) GPS receiver. Deterministic corrections based either on single-element or array calibration (and implemented as a line-of-sight-based lookup table) will reduce pseudorange and carrier-phase biases in the tracking output. For the STAP algorithms and patch-element-based antenna array considered here, the carrier-phase bias residuals are on the order of 0-10° and the pseudorange bias residuals are in the 10's of cm. While the carrier-phase residuals are likely tolerable for high-integrity carrier-phase-differential integer resolution, the code-phase residuals are troubling and will need further work in regards either to algorithm development, to antenna design improvements, or to both.

INTRODUCTION

The Joint Precision and Approach Landing System (JPALS) is a United States Navy and Air Force program to provide local-area augmentation to the on-board GPS navigation solution for pilots on approach to aircraft carrier, fixed-base, and tactical airfields. Sea-based JPALS provides carrier-phase-differential navigation, and

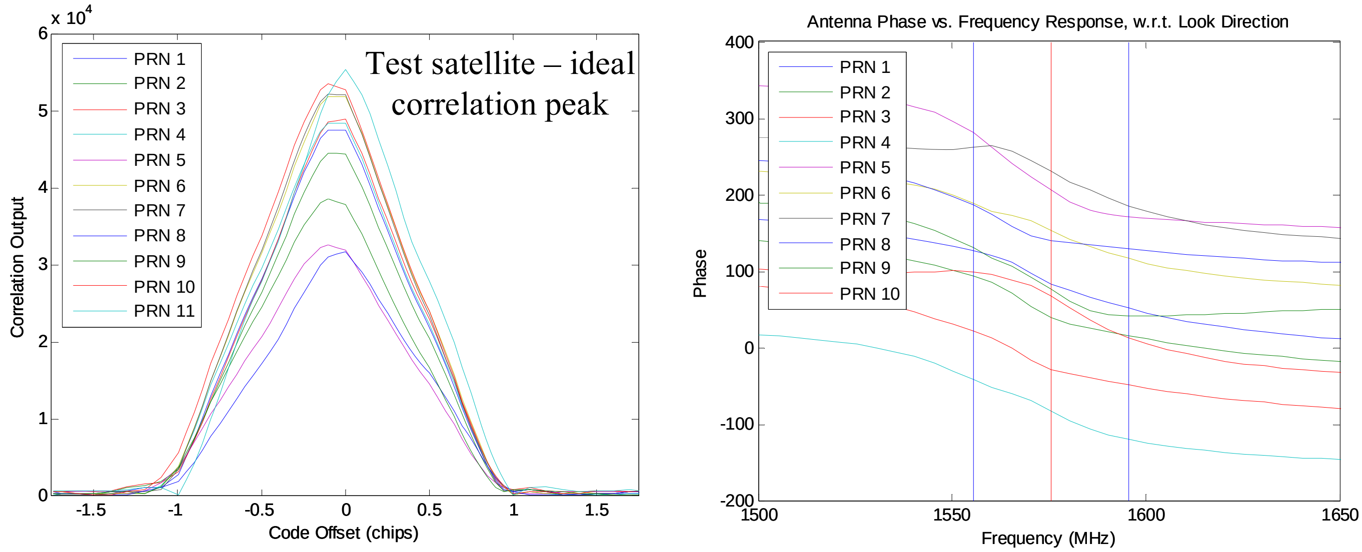

Figure 1. Antenna gain/phase response varies as a function of incoming signal azimuth, elevation, and frequency – L1 microstrip patch antenna [2].
Left: correlation peak distortion. Right: carrier-phase bias.

as such there is the requirement to maintain high-integrity GPS measurements while simultaneously rejecting radio frequency interference (RFI) and multipath. To increase the available C/No, the baseline JPALS architecture includes a multi-element antenna array. Adaptive beamsteering and nullforming are being studied to further improve interference rejection.

Unlike the response of an ideal isotropic element, that of a single-element fixed reception pattern antenna (FRPA) varies as a function of incoming signal azimuth, elevation, and frequency. This distortion leads to biases in code-phase (pseudorange) and carrier-phase, and possibly to attenuation of the incoming signal power (Figure 1 and Table 1). Bias errors, such as those shown in Table 1 for microstrip patch antennas developed at Stanford University [1], may be sufficient to make integer determination and carrier-phase-differential navigation problematic. In the GPS solution, the mean bias in pseudorange across all incoming signals is assigned to the user clock offset term; however, the residual pseudorange bias after this correction is still on the order of 2m. The carrier-phase bias needs to be a small fraction of a carrier cycle, which clearly is not the case for the microstrip patch antenna elements characterized here.

A multi-element antenna array may introduce additional biases in the pseudorange and carrier-phase estimates. Not only is this due to mutual electronic coupling between elements that does not exist for stand-alone antennas, but also it is a consequence of distortion that may be introduced by the spatial and temporal weighting in forming the composite array output signal.

Table 1. Antenna response and signal attenuation – L1 microstrip patch antenna [2].

Pseudorange and carrier-phase biases for the center antenna of a 7-element array, as a function of incoming signal line-of-sight; isotropic signal power of 40 dB-Hz.					
PRN	Incoming Signal Line-of-Sight		Pseudorange Bias (m)	Carrier-Phase Bias (deg)	C/No (dB-Hz)
	Az	El			
1	0	40	-2.0	85	37.5
2	30	30	-1.9	42	36.8
3	60	40	-1.5	-27	37.6
4	90	50	-2.3	-83	38.1
5	120	20	-2.8	-154	34.3
6	150	60	-2.2	154	38.7
7	210	70	-2.4	-129	38.9
8	240	20	-0.5	141	33.6
9	270	30	-3.0	76	35.9
10	300	80	-2.7	67	38.8

In order to increase the probability of correctly fixing integer ambiguities during carrier-phase-differential navigation, some form of bias mitigation is necessary. This could be implemented, for example, by frequency-domain equalization or by a line-of-sight-based bias calibration look-up table [2]. Equalization could take the form of appropriate filtering of the incoming satellite signals to undo the distortion caused by the antenna gain and phase response, and therefore would apply to any subsequent method of calculating antenna weights. However, since the antenna response is a strong function of the incoming signal line-of-sight, the filter coefficients would likewise be line-of-sight dependent, requiring a massive database of filter coefficient terms. An alternative approach would be to apply deterministic pseudorange and carrier-phase corrections to the tracking output quantities themselves – the corrections would be stored in a look-up table and tagged according to the incoming signal line-of-sight. The look-up table approach applies corrections for only one set of antenna weights. Because this mitigation method is simpler to implement and verify, it is considered preferable to frequency-domain equalization and is the method studied in the remainder of this report.

In non-adaptive spatial-only beamsteering the beamsteering weights are calculated deterministically based on satellite position and array orientation. Consequently, biases may be eliminated with a precise look-up table, namely pseudorange and carrier-phase corrections tagged to incoming signal line-of-sight (Figure 2). The use of multiple antennas inherently improves C/No relative to the single antenna case. However, the drawbacks of a deterministic controlled reception pattern antenna array (CRPA) include high sidelobes and uncontrolled nulls that may not effectively reject incoming interference or signal multipath.

Adaptive processing for noise-rejection or power-minimization allows the automatic suppression of narrowband interference [3-4] but may exacerbate bias errors compared to deterministic weighting. The reason for the modified biases is that adaptive weighting of single-element distortion from the slave antennas shifts the pseudorange and carrier-phase measurements. Even greater interference rejection, particularly of wideband sources, may be realized by incorporating temporal filtering in the array processing – e.g., with a tapped delay line antenna array [5-9]. However, adding time taps to allow space-time adaptive processing (STAP) yields a finite impulse response filter that may further distort the spread-spectrum GPS ranging signal [10-11].

This paper evaluates the trade-offs between pseudorange and carrier-phase bias errors and RFI rejection in adaptive, multi-antenna GPS receivers. To this end, array performance was evaluated with regards to both code- and carrier-phase estimation errors as well as tracking output signal-to-noise ratio. Adaptive algorithms that were considered in this study include:

1) A least-mean-square (LMS) error approach to weight vector determination that seeks to

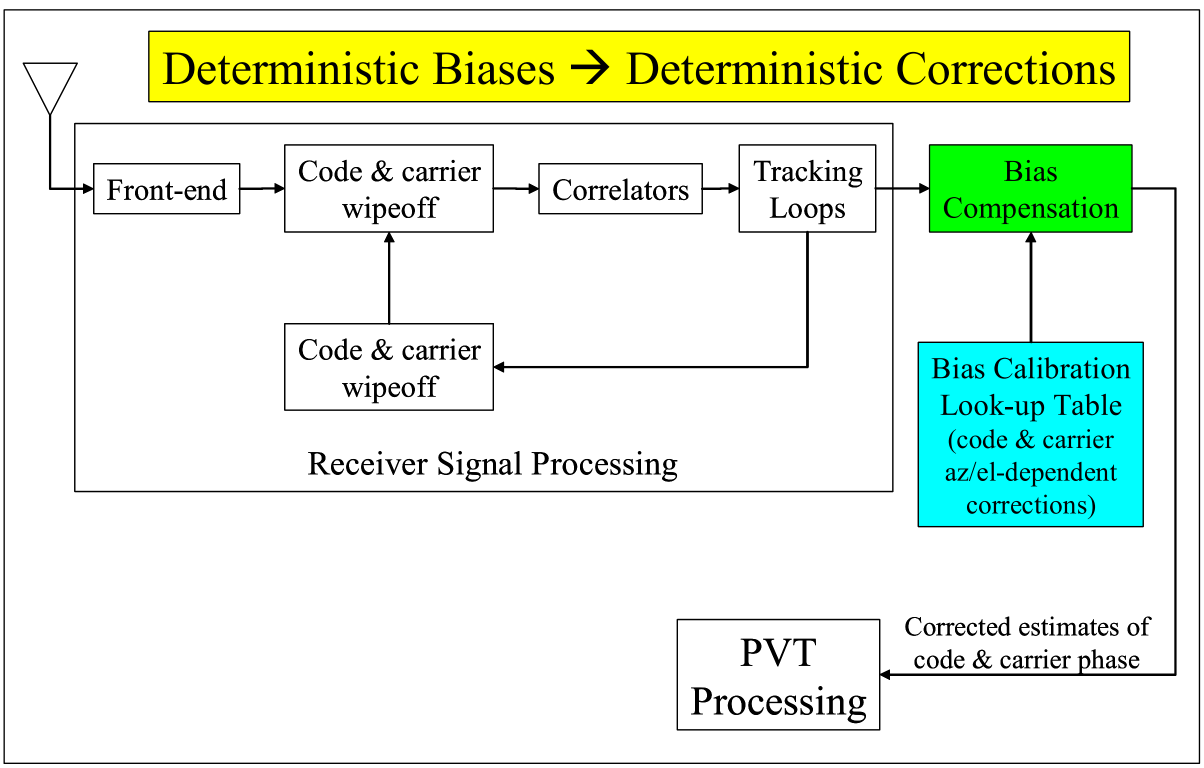

Figure 2. Pseudorange and carrier-phase bias compensation.

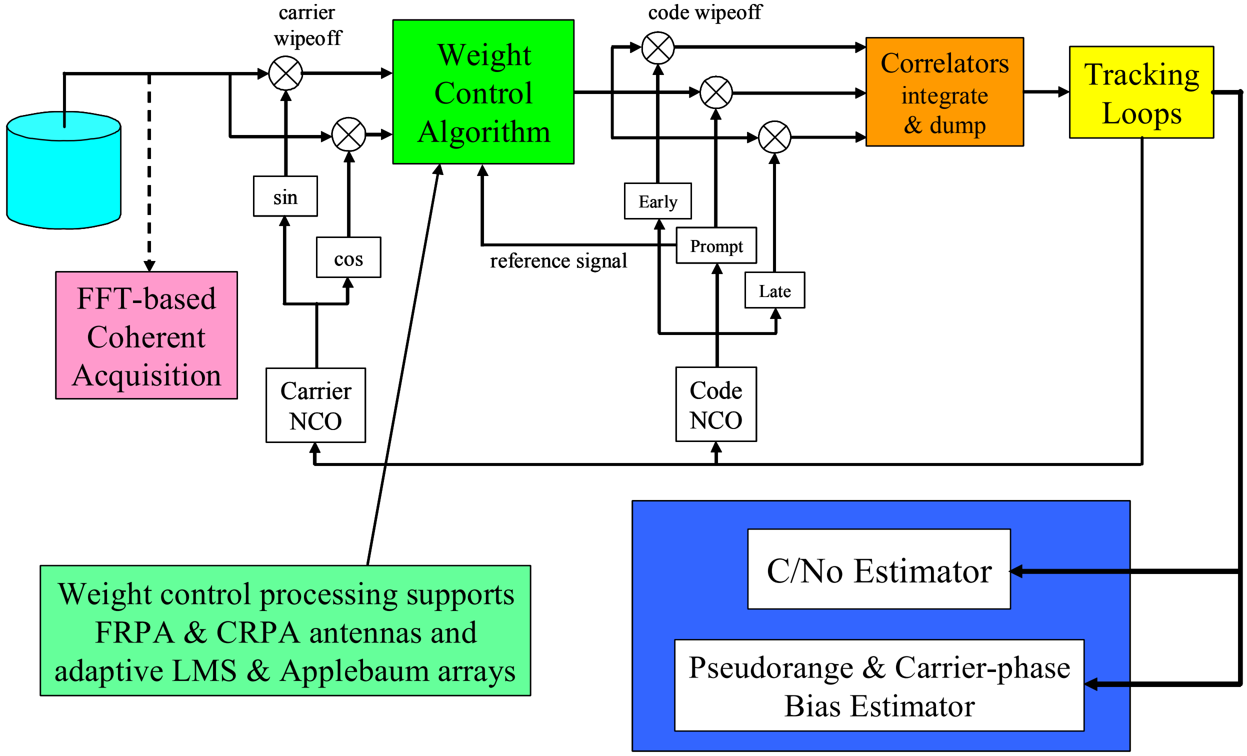

Figure 3. Software receiver block diagram.

minimize the difference between the actual array output and the value of a pilot or reference signal – this approach can also be termed blind-adaptive beamsteering/nullforming, since no knowledge of incoming signal line-of-sight or array geometry is required [12-13].

2) A steering-vector-based (Applebaum) approach that constrains the array response in the direction of the arriving signal (neglecting for the moment the effects of antenna distortion in the calculation of the weight vector) and then seeks to minimize the remaining array output power [14-15].

These algorithms were developed as part of a software-based, all-in-view GNSS receiver that is capable of tracking either simulated or actual satellite signals (Figure 3). In conjunction with this software receiver, a signal simulation environment was created that allows generation of GPS C/A-code or P-code signals incident on a multi-element array, as well as injection of narrow-band or wide-band interference. An important feature of this simulator is the ability to incorporate electronic models of the gain and phase response of the various antennas in the array as a function of incident signal arrival direction (Figure 4).

Using this signal simulation environment and software receiver, it is possible to show the advantages of adaptive arrays with respect to RFI rejection, and to quantify their pseudorange and carrier-phase bias residuals after suitable look-up table corrections are applied. Deterministic corrections based either on single-element or array calibration (and implemented as a line-of-sight-based lookup table) will reduce pseudorange and carrier-phase biases in the tracking output. For the STAP algorithms and patch-element-based antenna array considered here, the carrier-phase bias residuals are on the order of 0-10° and the pseudorange bias residuals are in the 10's of cm. While carrier-phase residuals are likely tolerable for high-integrity carrier-phase-differential integer resolution, the code-phase residuals are troubling and will need further work in regards either to algorithm development, to antenna design improvements, or to both.

METHODOLOGY

Antennas introduce biases in the estimates of code-phase and carrier-phase due to their variation in response as a function of incoming signal azimuth, elevation, and frequency. Multi-element antenna arrays, while increasing C/No and nulling/rejecting RFI, may compound these distortion-induced biases. If the weights themselves are deterministic functions of satellite and array geometry, then the biases are likewise deterministic. However, if the weights are calculated adaptively, then the biases are determined by the signal environment, STAP algorithm, and receiver tracking implementation. Therefore, in order to evaluate pseudorange and carrier-phase corrections, or the bias residuals after deterministic compensation, it is necessary to evaluate receiver

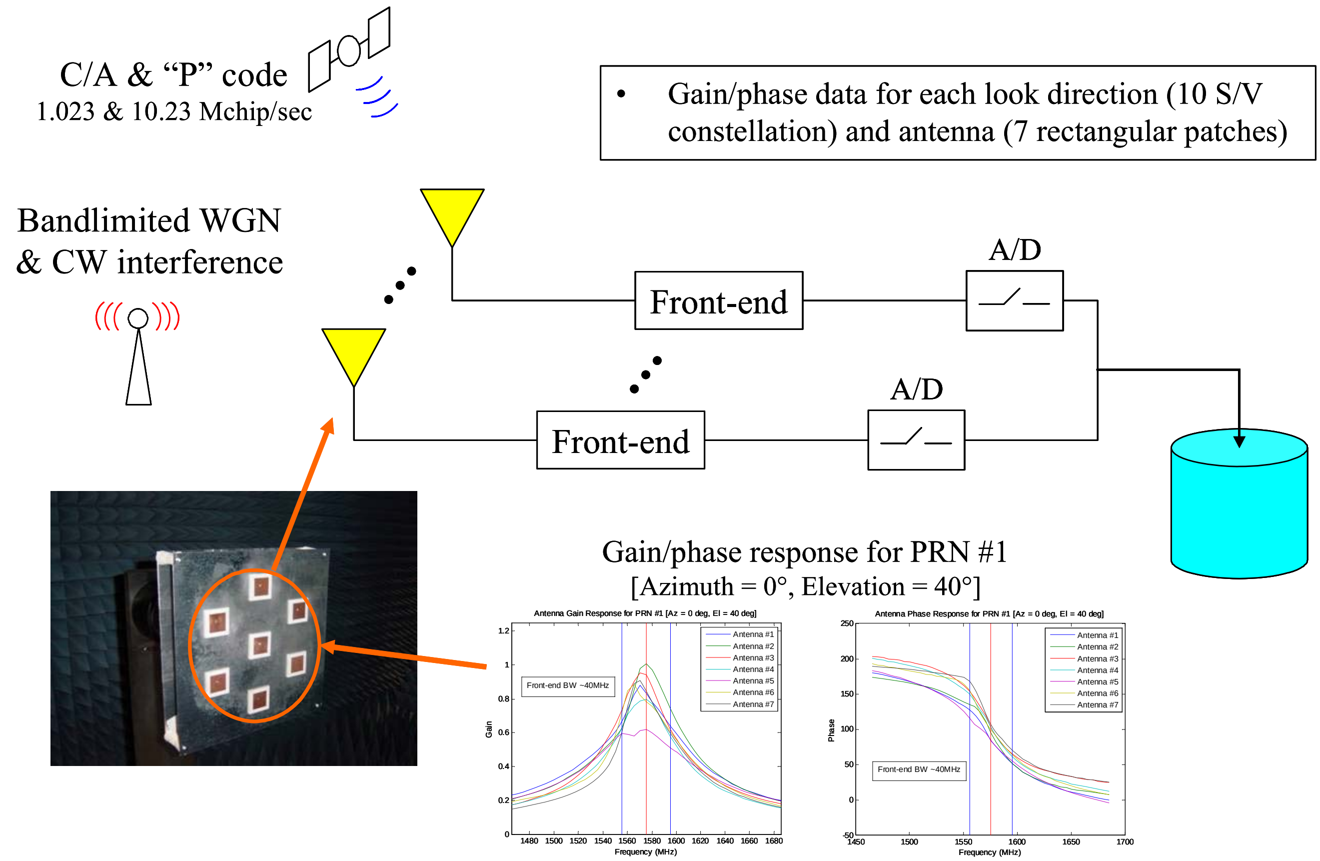

Figure 4. Software-based signal simulator – models satellite signal reception, correlated interference, non-correlated, Gaussian noise, and antenna-induced signal distortion.

performance in the context of realistic GPS tracking scenarios. This dictates an end-to-end study that encompasses antenna characterization, signal/RFI generation, adaptive weight computation, and signal tracking. Then, the receiver estimates of the tracking observables (code-phase, carrier-phase, and C/No) may be compared to the truth values from the signal simulator. With all variables under direct control, this allows isolation and estimation of the parameters of interest.

A software signal generator, as shown in Figure 4, was developed to produce P-code-like signals mixed-down from the GPS-L1 frequency to a suitable intermediate frequency for sampling (f_S = 80MHz, f_{IF} = 20MHz, front-end bandwidth of 40MHz). The spreading-code modulation used the P-code generator and a chipping rate of 10.23 Mchips/sec, but short-cycled after the first millisecond to make implementation of the tracking code more straightforward. Time-offsets based on incoming signal line-of-sight and array geometry were applied to advance or retard the received signal with respect to the array physical center; the array comprised a center master element and a hexagonal pattern of slave elements with $\lambda/2$ baselines. A "standard constellation" of 10 satellites was used (Figure 5), with locations selected to correspond to previously-identified extremes in the code/carrier bias maps. The ratio of signal to white Gaussian noise (WGN) was set to deliver a C/No of 40 dB-Hz for an isotropic receiving element; this noise is not correlated across antenna elements. In addition, there is wideband interference incident on the array – this interference is correlated in space/time between the various elements of the array. The RFI emitters are placed at or near the horizon, and the power level can be varied to achieve the desired jammer-to-signal (J/S) power ratio.

The signal generator code also simulated signal distortion introduced by the multi-element antenna array. The GPS signals were received either by an array of isotropic antenna elements or by a 7-element array whose gain and phase response characteristics were as determined by previous electronic simulation models and anechoic chamber measurements [2]. The method of incorporating the gain and phase characteristics is by frequency-domain convolution with the generated satellite signals. Finally, real-valued samples are stored to disk at 4-bit resolution, after passing through an automatic gain-control stage to ensure good dynamic range performance.

The generated signals were then fed as inputs into a software-based GNSS receiver (Figure 3). This receiver uses standard PLL and DLL tracking loops, and has the

PRN	Azimuth	Elevation
1	0	40
2	30	30
3	60	40
4	90	50
5	120	20
6	150	60
7	210	70
8	240	20
9	270	30
10	300	80

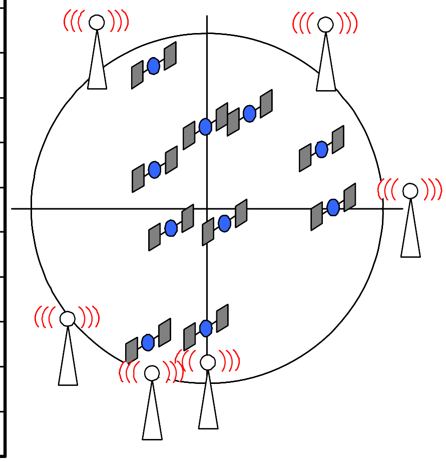

RFI	Azimuth	Elevation
1	0	0
2	45	0
3	120	0
4	225	0
5	250	0
6	270	10

Figure 5. Satellite and RFI constellation.

capability of tracking either GPS C/A code, pseudo P-code originating from the previously described signal simulator, or Galileo signals recorded from the GIOVE-A satellite either on the L1, E5, or E6 bands. The receiver is a flexible, all-in-view, MATLAB™ implementation, which incorporates some organizational and data-structure elements from other publicly-available code bases [16].

Distinguishing this receiver implementation is the inclusion of array-processing modules, either for deterministic beamsteering or for adaptive beamsteering and nullforming using space/time adaptive processing. Since the tracking outputs can be compared directly with the known code-phase and carrier-phase input values from the signal simulator, it is possible to determine precisely the corresponding pseudorange and carrier-phase biases due to antenna-induced distortion effects and array processing. Likewise, the software receiver can estimate the C/No ratio for the received signal, which allows quantification of the noise/RFI performance of the various array processing approaches (Figure 6).

In determining pseudorange and carrier-phase biases, it is important to suppress the effects of noise in the output signal to obtain a precise estimate. Because the pseudorange standard deviation shown in Figure 6 is in the 10's of centimeters, substantial filtering would be needed to attenuate the noise effects. Instead, a two-step process is implemented to first track the signals in the presence of WGN (noise uncorrelated across elements) and RFI (correlated interference) while updating the antenna weights based on the selected adaptation scheme (Figure 7a), and then second to track the signals without WGN or RFI, while playing back the stored weight vector from the previous step at each processing epoch (Figure 7b). In this way, bias values may be computed directly from a short-duration simulation (Figure 8).

RESULTS

The first important result from the signal simulation and tracking process is the characterization of the RFI-free pseudorange and carrier-phase biases and C/No performance of the non-ideal single-element FRPA, the 7-element deterministic CRPA, and the

Table 2. Uncompensated code-phase and carrier-phase biases.

Uncompensated pseudorange and carrier-phase biases; isotropic signal power of 40 dB-Hz.				
Averages over 10-satellite constellation	Single-element FRPA	7-element deterministic CRPA	Blind-adaptive STAP beam/null steering (LMS-based)	Steering-vector STAP beam/null steering (Applebaum-based)
Pseudorange bias (m)	2.13	1.88	1.94	1.88
Carrier-phase bias (deg)	96	96	96	96
C/No (dB-Hz)	37.0	45.7	45.7	45.7

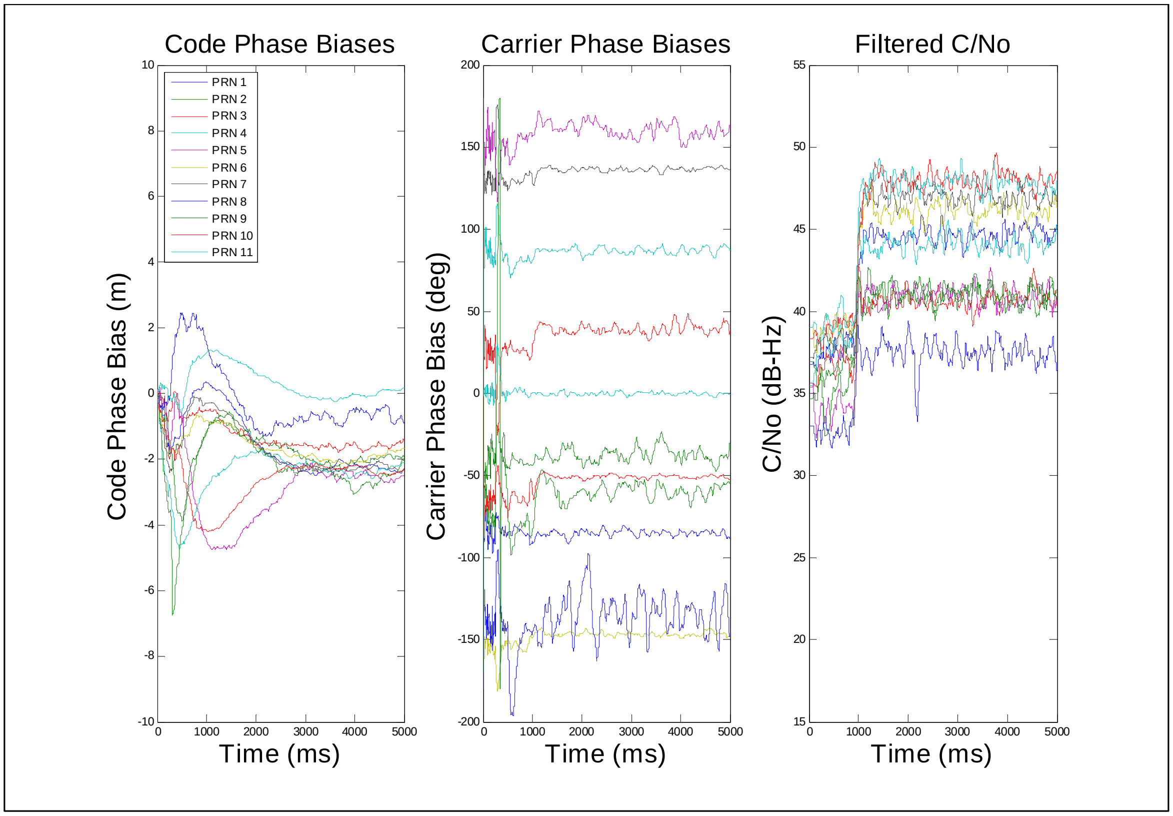

Figure 6. Software receiver tracking output and noise/bias estimation;
Applebaum-based STAP, C/No = 40 dB-Hz plus six RFI sources at J/S = 30dB.

beamsteering/nullforming adaptive arrays (Table 2). The bias levels are clearly unacceptable for carrier-phase-differential integer resolution and navigation. For the antenna array studied, there is an average code-phase bias due to correlation peak distortion of approximately 2m (standard deviation ~70cm). The corresponding carrier-phase biases are essentially uniformly distributed from -180 to +180 degrees.

As expected, the multi-element antennas achieved better C/No than the single-element FRPA. Carrier-to-noise ratio was evaluated taking non-ideal antenna effects into account (Figure 4). For this RFI-free case, the thermal noise level was set so that an ideal isotropic antenna would achieve a C/No of 40 dB-Hz. The attenuation of signal energy due to non-ideal gain response of the single-

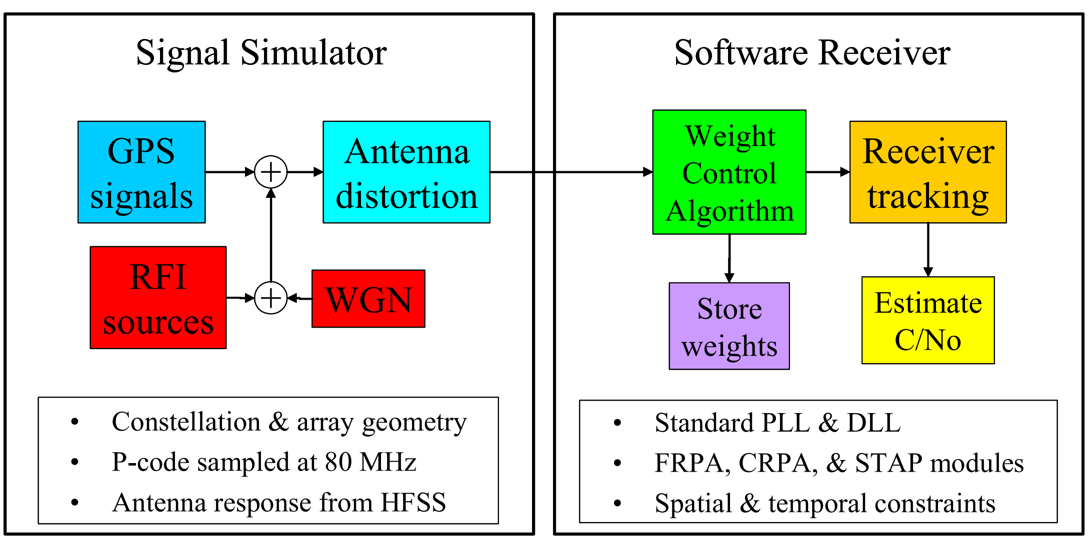

Figure 7a. Methodology for estimating code/carrier biases and C/No.

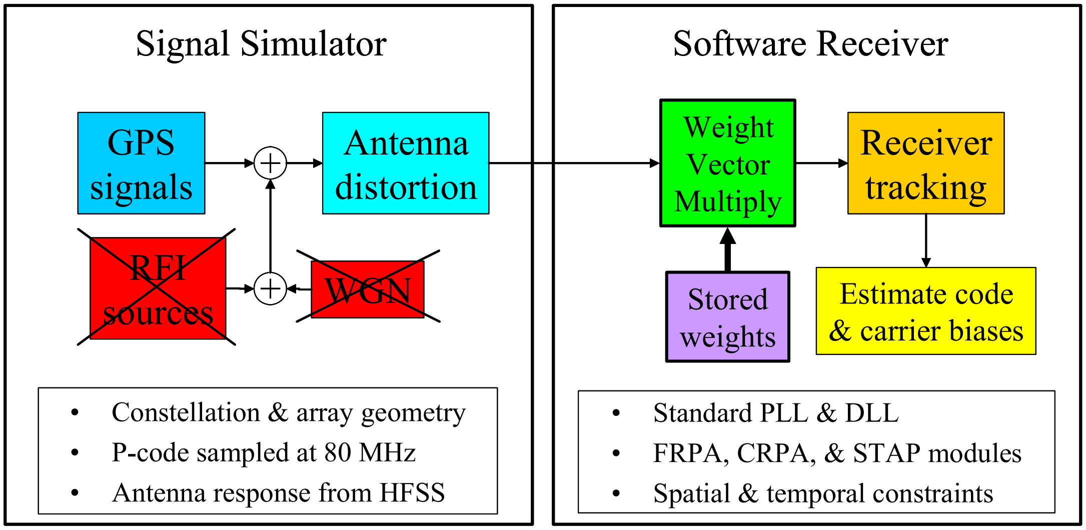

Figure 7b. Methodology for estimating code/carrier biases and C/No.

element FRPA results in tracked C/No of about 3 dB-Hz below the 40 dB-Hz level that would be produced for an isotropic antenna. All of the multi-element arrays yield ~8.5 dB-Hz improvement in C/No [10*log10(7) = 8.5 dB] with respect to the single-element FRPA. The response of the adaptive arrays closely matches the deterministic case, since in the absence of RFI the converged (steady-state) adaptive weight vector solutions approach that of the deterministic CRPA.

RFI-free simulations also revealed that different types of look-up tables should be used for different CRPA

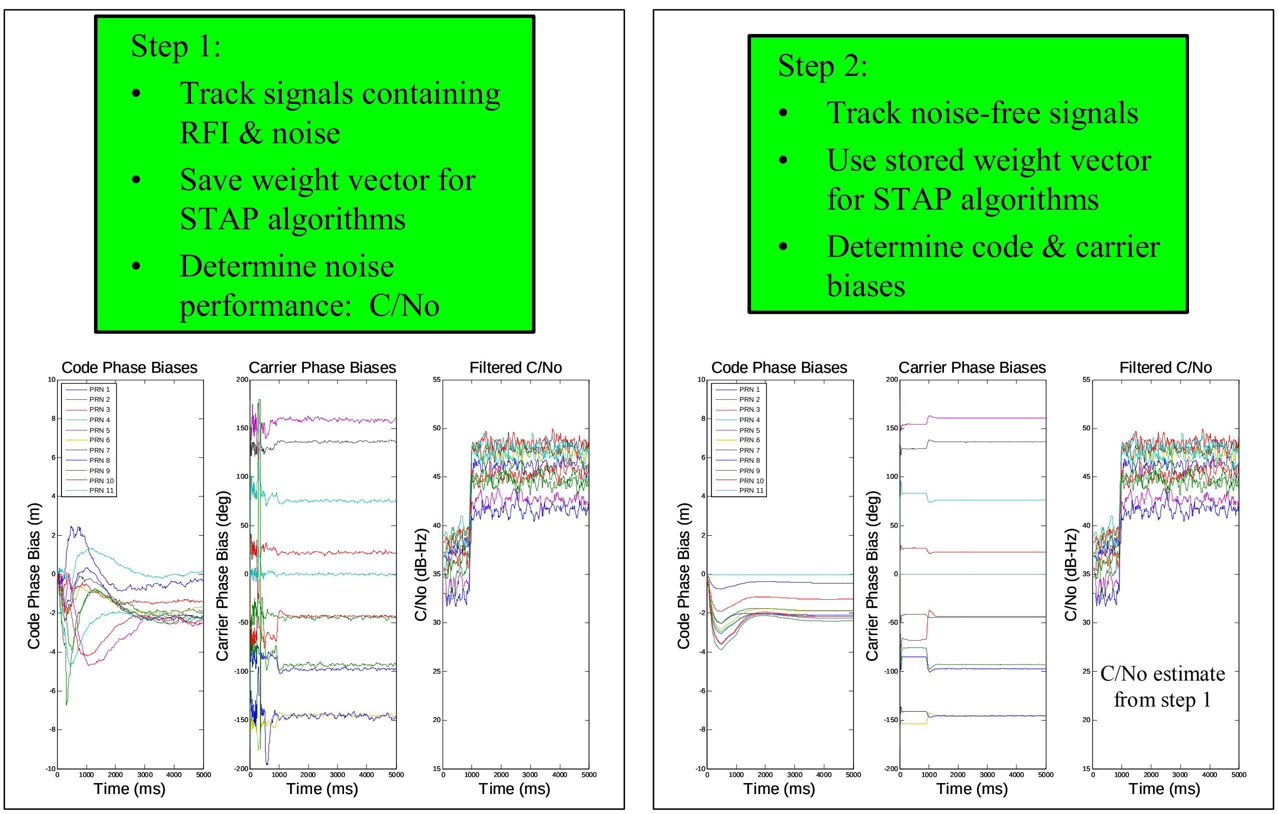

Figure 8. Two-step process for estimating C/No and code/carrier biases in presence of noise/RFI. This example shows 7-antenna, Applebaum-based space-time adaptive processing (with a single time-tap), C/No of 40 dB-Hz, plus six RFI sources at J/S of 30dB.

Table 3. Bias residuals after compensation – the best calibration option depends on STAP algorithm.

Pseudorange and carrier-phase biases; isotropic signal power of 40 dB-Hz.			
Averages over 10-satellite constellation		Blind-adaptive STAP beam/null steering (LMS-based)	Steering-vector STAP beam/null steering (Applebaum-based)
Bias residuals w.r.t. single-element FRPA calibration	Pseudorange bias (m)	0.23	0.28
	Carrier-phase bias (deg)	0.5	9.2
Bias residuals w.r.t. 7-element CRPA calibration	Pseudorange bias (m)	0.06	0.00
	Carrier-phase bias (deg)	9.3	0.0

algorithms. As discussed previously, a look-up table of pseudorange and carrier-phase biases could be calibrated for either the single-element FRPA or the deterministic CRPA, reducing the antenna-induced navigation biases to zero. Either of these two look-up table compensation strategies could be applied for use with adaptive weighting algorithms. Because these look-up strategies are tuned for specific weight vector combinations, however, some calibration error is expected when a static look-up table is used with an adaptive algorithm.

Of the FRPA and CRPA deterministic look-up corrections, the better compensation option depends on the adaptive algorithm (the blue-shaded cells in Table 3). For LMS-based blind/adaptive beamsteering/nullforming, pseudorange bias corrections should come from the deterministic CRPA calibration, while the carrier-phase corrections should come from the single-element FRPA calibration. The reason for the near-zero carrier-phase bias with respect to the single-element FRPA is that the weight adjustment algorithm seeks to steer all desirable incoming signal energy to the in-phase channel of the master element. For Applebaum-based steering-vector beamsteering/nullforming, both pseudorange and carrier-phase corrections should come from the deterministic CRPA calibration. The reason for the effectiveness of this compensation scheme in the RFI-free case is that the converged weight vector is identical to that of the deterministic CRPA.

By comparing high-RFI simulations (J/S = 50dB for each of six wideband RFI emitters) to the RFI-free case, it is possible to define the trade-offs between bias and noise performance for various adaptive weighting schemes (Figure 9). In Figure 9, the horizontal axis shows the improvement in C/No for the adaptive algorithms with respect to the deterministic CRPA for the RFI-free and high-RFI conditions, while the vertical axis shows the increase in pseudorange and carrier-phase bias after bias compensation. It should be noted that more noise rejection and lower biases are to be desired – this corresponds to movement in Figure 9 down and to the right. While in the RFI-free case the C/No performance of the adaptive arrays matches that of the deterministic CRPA, the presence of RFI causes the adaptive arrays to clearly outperform the deterministic CRPA. This is demonstrated by the C/No improvement for the STAP algorithms with respect to the deterministic CRPA when including six 50dB RFI emitters (i.e., J/S for each emitter is 50 dB). The increase in C/No with respect to the deterministic CRPA comes at the expense of greater pseudorange and carrier-phase biases; this is shown in Figure 9 as the increase in pseudorange and carrier-phase bias residual after compensation for the six RFI emitter case.

Neither the LMS-based nor Applebaum-based algorithms clearly outperform to other in all respects. Figure 9 clearly shows that steering-vector-based STAP (the Applebaum approach) yields better carrier-phase performance than blind-adaptive beamsteering and nullforming (the LMS approach) in the presence of RFI when calibration data are available. However, blind-adaptive STAP has better RFI rejection capability than the steering-vector-based method for the scenario herein described, i.e. 10dB vs. 8dB C/No improvement with respect to the deterministic CRPA, or a 2dB advantage. Both STAP approaches produce comparable code-phase bias residuals.

CONCLUSION

This paper has evaluated the trade-offs between pseudorange and carrier-phase bias errors and RFI rejection in adaptive, multi-antenna GPS receivers. Deterministic corrections based either on single-element

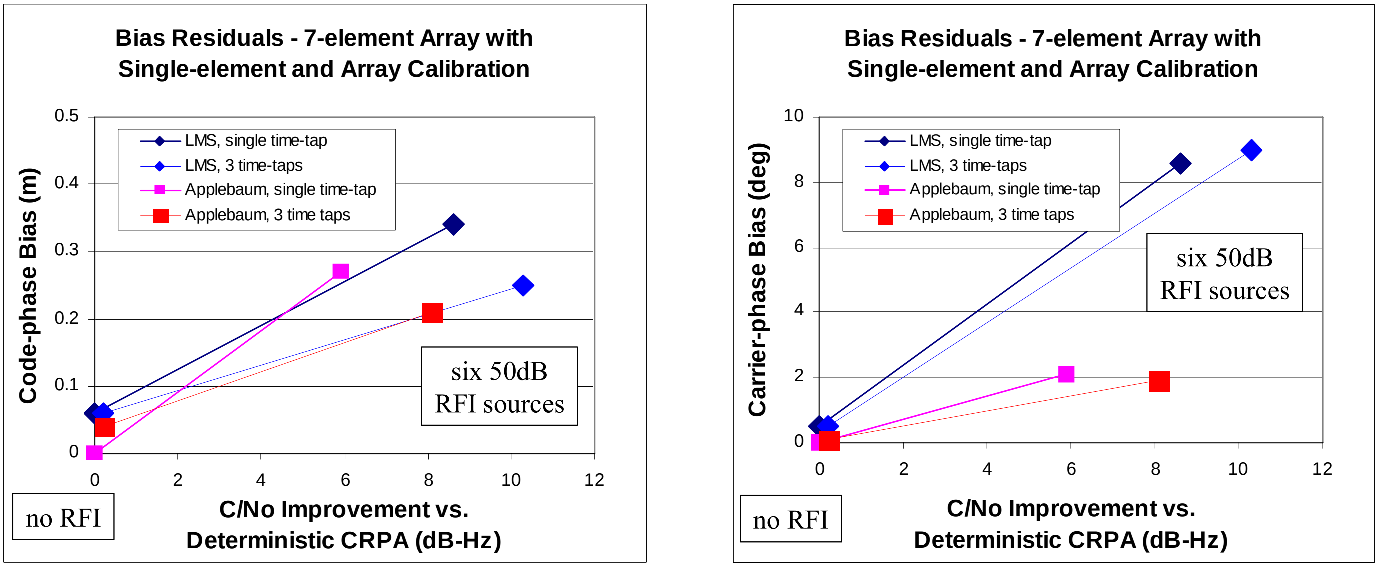

Figure 9. Bias residuals and C/No improvement for STAP arrays with respect to a 7-element deterministic beamsteering array.

or array calibration (and implemented as a line-of-sight-based lookup table) reduce pseudorange and carrier-phase biases in the tracking output. For the STAP algorithms and patch-element-based antenna array considered here, the carrier-phase bias residuals are on the order of 0-10° and the pseudorange bias residuals are in the 10's of cm. While carrier-phase residuals are likely tolerable for high-integrity carrier-phase-differential integer resolution, the code-phase residuals are troubling and will need further work in regards either to algorithm development, to antenna design improvements, or to both.

There is significant future relevance to the work described here, not only for military landing systems but also for civilian receivers operating with next-generation GNSS signals. This is due to the facts that pseudorange and carrier-phase biases are a strong function of the spreading-code bandwidth and that military and next-generation signals have higher code chipping rates than the current GPS C/A code rate of 1.023 Mchips/sec. In addition, the increased attention paid to denial-of-service due to unintentional or harmful RFI makes STAP algorithms desirable for safety-of-life applications.

ACKNOWLEDGMENTS

The authors gratefully acknowledge the support of the JPALS Program Office, and the Naval Air Warfare Center Aircraft Division through contract N00421-05-C-0068.

REFERENCES

1. Kim, U.S., 2006, "Mitigation of Signal Biases Introduced by Controlled Reception Pattern Antennas in a High Integrity Carrier Phase Differential GPS System," PhD dissertation defense, Stanford University.
2. Kim, U.S., 2005, "Analysis of Carrier Phase and Group Delay Biases Introduced by CRPA Hardware," *Proc. ION GNSS 2005*.
3. Gecan, A. and Zoltowski, M., 1995, "Power Minimization Techniques for GPS Null Steering Antenna," *Proc. ION GPS 1995*, pp. 861-868.
4. Nicholson, B.W., Upton, D.M., Cotterill, S., Marchese, J., Upadhyay, T., and Vander Velde, W.E., 1998, "Computer Simulations of Digital Beam Forming Adaptive Antennae for GPS Interference Mitigation," *Proc. ION NTM 1998*, pp. 355-360.
5. Hatke, G.F., 1998, "Adaptive Array Processing for Wideband Nulling in GPS Systems," *Proc. Thirty-Second Asilomar Conf. on Signals, Systems & Computers*, vol. 2, pp. 1332-1336.
6. Fante, R.L. and Vaccaro, J.J., 2000, "Wideband Cancellation of Interference in a GPS Receive Array," *IEEE Trans. on Aerospace and Electronic Systems*, vol. 36, no. 2, pp. 549-564.
7. Gupta, I.J. and Moore, T.D., 2001, "Space-Frequency Adaptive Processing (SFAP) for Interference Suppression in GPS Receivers," *Proc. ION NTM 2001*, pp. 377-385.
8. Moore, T.D., 2002, "Analytic Study of Space-Time and Space-Frequency Adaptive Processing for Radio Frequency Interference Suppression," PhD. Dissertation, The Ohio State University.

9. Hatke, G.F. and Phuong, T.T., 2004, "Design and Test of a GPS Adaptive Antenna Array Processor: The Multipath Adaptive Multibeam Array (MAMBA) Processor," Lincoln Laboratory Project Report GPS-16, Massachusetts Institute of Technology.
10. Fante, R.L., Fitzgibbons, M.P., and McDonald, K.F., 2004, "Effect of Adaptive Array Processing on GPS Signal Crosscorrelation," *Proc. ION GNSS 2004*, pp. 579-583.
11. McGraw, G.A., Ryan Young, S.Y., and Reichenauer, K., 2004, "Evaluation of GPS Anti-Jam System Effects on Pseudorange and Carrier Phase Measurements for Precision Approach and Landing," *Proc. ION GNSS 2004*, pp. 2742-2751.
12. Widrow, B., Mantey, P.E., Griffiths, L.J., and Goode, B.B., 1967, "Adaptive Antenna Systems," *Proc. IEEE*, vol. 55, no. 12, pp. 2143-2159.
13. Widrow, B. and Stearns, S.D., 1985, Adaptive Signal Processing, Pearson Education, Inc.
14. Applebaum, S.P., 1976, "Adaptive Arrays," *IEEE Trans. on Antennas and Propagation*, vol. 24, no. 5, pp 585-598.
15. Compton, R.T., 1988, Adaptive Antennas, Prentice-Hall, Inc.
16. Borre, K., Akos, D.M., Bertelsen, N., Rinder, P., and Jensen, S.H., A Software-Defined GPS and Galileo Receiver: A Single-Frequency Approach, Birkhauser, in press.